Generation of an Active Monomer of Rabbit Muscle Creatine Kinase by Site-Directed Mutagenesis: The Effect of Quaternary Structure on Catalysis and Stability†

Julia M. Cox, Caroline A. Davis, Chikio Chan, Michael J. Jourden, Andrea D. Jorjorian, Melissa J. Brym, Mark J. Snider, Charles L. Borders, Jr., and Paul L. Edmiston*

Department of Chemistry, The College of Wooster, Wooster, Ohio 44691

Received October 29, 2002; Revised Manuscript Received December 17, 2002

ABSTRACT: Cytosolic creatine kinase exists in native form as a dimer; however, the reasons for this quaternary structure are unclear, given that there is no evidence of active site communication and more primitive guanidino kinases are monomers. Three fully conserved residues found in one-half of the dimer interface of the rabbit muscle creatine kinase (rmCK) were selectively changed to alanine by site-directed mutagenesis. Four mutants were prepared, overexpressed, and purified: R147A, R151A, D209A, and R147A/R151A. Both the R147A and R147A/R151A were confirmed by size-exclusion chromatography and analytical ultracentrifugation to be monomers, whereas R151A was dimeric and D209A appeared to be an equilibrium mixture of dimers and monomers. Kinetic analysis showed that the monomeric mutants, R147A and R147A/R151A, showed substantial enzymatic activity. Substrate binding affinity by R147A/R151A was reduced approximately 10-fold, although k_{cat} was 60% of the wild-type enzyme. Unlike the R147A/R151A, the kinetic data for the R147A mutant could not be fit to a random-order rapid-equilibrium mechanism characteristic of the wild-type, but could only be fit to an ordered mechanism with creatine binding first. Substrate binding affinities were also significantly lower for the R147A mutant, but k_{cat} was 11% that of the native enzyme. Fluorescence measurements using 1-anilinonaphthalene-8-sufonate showed that increased amounts of hydrophobic surface area are exposed in all of the mutants, with the monomeric mutants having the greatest amounts of unfolding. Thermal inactivation profiles demonstrated that protein stability is significantly decreased in the monomeric mutants compared to wild-type. Denaturation experiments measuring λ_{max} of the intrinsic fluorescence as a function of guanidine hydrochloride concentration helped confirm the quaternary structures and indicated that the general unfolding pathway of all the mutants are similar to that of the wild-type. Collectively, the data show that dimerization is not a prerequisite for activity, but there is loss of structure and stability upon formation of a CK monomer.

In the native state, three mammalian cytosolic isoenzymes of creatine kinase (CK[1,2] EC 2.7.3.2) are composed of two distinct gene products, the muscle (M) and/or brain (B) forms that exist exclusively as 86 kDa dimers (MM, BB, or MB) (*1*). Each subunit of CK reversibly catalyzes the transfer of a phosphate between MgATP and the guanidino group of creatine to generate MgADP and phosphocreatine allowing cells which require large energy fluxes (i.e., brain, heart, or muscle) to rapidly regenerate ATP from stored supplies of phosphocreatine during periods of high activity. Since the first report of its purification from rabbit muscle (*2*), CK has been the subject of numerous studies of its physicochemical properties and catalytic mechanism (*3*−*5*). Despite its dimeric structure, there has been no coopertivity observed between the two active sites of rabbit muscle CK (rmCK) based on kinetic analysis (*6*, *7*) although it is unknown if the single active site located on each subunit acts in complete independence of the other. No allosteric regulation mechanisms of CK have been found or postulated. Thus, the regulatory advantages concomitant with enzyme oligomerization do not appear to be exploited by cytosolic CK.

Creatine kinase, which is found primarily in vertebrates (*3*, *8*), belongs to a larger family of phosphogen kinases that use a substrate containing a guanidino group. Another prominent member of this group of enzymes is arginine kinase (AK), which is found most often in invertebrates (*8*). Based on analysis of a sequence database of guanidino kinases, it appears that CK and AK diverged far in the

† This work was supported by NSF Grant #9982401 (C.L.B. and P.L.E.) and Scholar/Fellow Award #SF-96-001 from the Camille and Henry Dreyfus Foundation (C.L.B. and P.L.E.).

* To whom correspondence should be addressed. E-mail: pedmiston@wooster.edu. Telephone: (330) 263-2113. Fax: (330) 263-2386.

[1] Abbreviations: AK, arginine kinase; ANS, 1-anilinonaphthalene-8-sufonate; AUC, analytical ultracentrifugation; B, brain isoform; BSA, bovine serum albumin; CK, creatine kinase; DTT, dithiothreitol; EDTA, ethylenediaminetetraacetic acid; FPLC, fast protein liquid chromatography; GdnHCl, guanidine hydrochloride; IPTG, isopropyl β−D-1-thiogalactopyranoside; LB, Luria broth; M, muscle isoform; MES, 2-(N-morpholino)ethanesulfonate; PMSF, phenylmethanesulfonyl fluoride; rmCK, rabbit muscle creatine kinase; SEC, size exclusion chromatography; TE, 20 mM Tris, 0.1 mM EDTA, pH 8.00; TES, N-[tris(hydroxymethyl)methyl]-2-aminoethanesulfonate; Tris, tris(hydroxymethyl)-aminomethane; WT, wild-type rmCK.

[2] All CK residues are numbered using the sequence of rabbit muscle CK reported elsewhere (*18*, *28*).

10.1021/bi027083b CCC: $25.00
Published on Web 01/28/2003

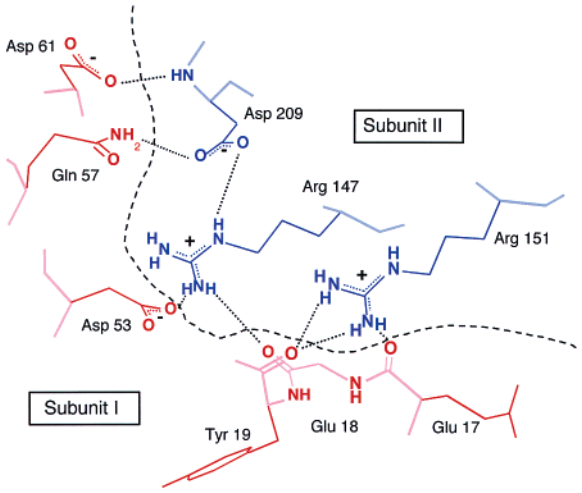

FIGURE 1: One contact region of the dimer interface of rmCK showing relevant interactions. Arg-151 makes three hydrogen bonds with the backbone carbonyls, two with Tyr-19 and one with Glu-17. Arg-147 makes a two hydrogen bonds across the interface with the backbone carbonyl of Glu-18 and the side chain carboxylate of Asp-53. A subunit−subunit hydrogen bond is made between carboxylate of Asp-209 and the side chain amide of Gln-57 and the backbone amide of Asp-209 and the carboxylate of Asp-61. An intrasubunit hydrogen bond is made between Arg-147 and the side chain of Asp-209. The rmCK dimer has 2-fold symmetry, so an identical contact region is duplicated elsewhere at the interface. Generated using SwissPDB Viewer and RasMol from PDB entry 2CRK (*15*).

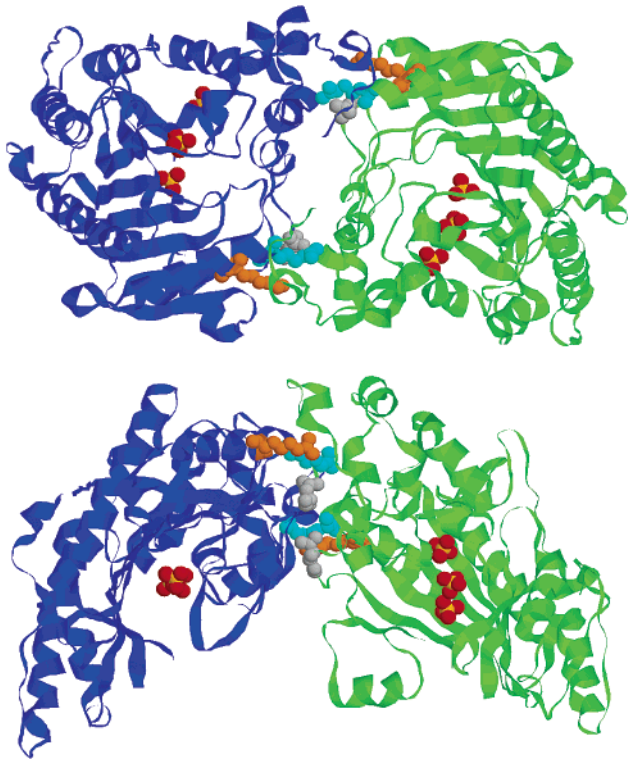

FIGURE 2: Two views of the X-ray crystal structure of the rmCK homodimer looking down on the dimer interface (top) and lengthwise along one active site cleft (bottom). The Arg-147 (orange), Arg-151 (cyan), and Asp-209 (grey) residues located at the interface are highlighted. Three sulfates bound in the putative MgATP binding site are shown in CPK colors. The regions of subunit contact are minimal, leaving an open space between the two monomers (top). The active sites are separated from the dimer interfaces by approximated 25 Å. Generated using SwissPDB Viewer and RasMol from PDB entry 2CRK (*15*).

evolutionary past (*9*). Due to the high level of sequence homology within the enzyme family, an unidentified ancestral guanidino kinase gene appears to have evolved to produce CK, AK, and the other phosphogen kinases (e.g., glycocyamine, taurocyamine, and lombricine kinase) found in a variety of multicellular organisms (*10*, *11*). In contrast to CK and other phosphogen kinases (i.e., glycocyamine kinase and lombricine kinase), AK exists as a monomer with rare exceptions (*12*). The first step in the evolution of a CK dimer may have been gene duplication since AKs from the sea anemone (*12*) and clam (*13*) are single ca. 80 kDa polypeptides containing two nonequivalent AK sequences. A gene duplicated CK also exists in the trematode (*14*). The evidence that CK may have evolved from a functional monomeric protein, combined with the lack of evidence of communication between CK active sites, has made the reasons for dimerization unclear.

On the basis of the X-ray crystal structure (*15*), two symmetrical contact areas of rmCK are relatively small and are bridged by polar interactions between residues E18, D53, Q57, and D61 from one subunit and S146, R147, R150, R151, and D209 from the other. R147, R151, and D209 each make three salt bridges or hydrogen bonding interactions within the dimer interface (Figure 1), and it has been suggested that these residues play an important role in dimer cohesion (*16*). W210, located near the interfacial contact region, has also been shown to be important for dimerization (*17*). Since the rmCK structure has exact 2-fold symmetry, the interactions shown in Figure 1 are duplicated within the dimer (Figure 2). Significantly, all the residues at the interface listed above except for E18 and S146 are fully conserved in all forms of CK (*18*). None of the corresponding residues mentioned are identical or conserved in monomeric AKs except for W210, which is fully conserved in all CK and AK enzymes (*18*).

Several workers have attempted to generate a catalytically active CK monomer using chemical denaturants to disrupt the interactions at the dimer interface. The first such report indicated that an active matrix bound monomer could be prepared under denaturing conditions (*19*). In a later study, Grossman et al. used urea to first completely denature MM-CK (*20*). The denaturant was rapidly diluted by addition to buffer, and it was noted that reactivation was complete prior to full reassociation, perhaps indicating the transient presence of active monomeric species. However, this conclusion was contradicted by the work of Vial who used NaCl and LiCl (*21*), sodium dodecyl sulfate (*22*), urea (*23*), and guanidine−HCl (*23*, *24*) to generate monomeric species of CK, none of which had measurable enzymatic activity. Whether or not inactivation was due to local denaturation of the active site prior to monomer formation could not be determined in these studies. However, experiments using covalently attached fluorescent probes (*25*) or spin-labels (*26*) in the active site region indicate that the active site is disrupted at low concentrations of denaturant and prior to large scale unfolding or dimer dissociation. The same conclusion is supported by denaturation experiments utilizing hydrodynamic pressure (*27*). As these results suggest, disruption of specific chemical interactions cannot be targeted by use of chemical denaturants and can lead to contradictory conclusions.

In the work reported herein, we have used site-directed mutagenesis to selectively eliminate several of the interactions at both dimer interface regions (rmCK is a homodimer). Five mutants of rmCK were prepared: R147A, R151A, D209A, R147A/R151A, and R147A/R151A/D209A. Site-directed mutagenesis is a powerful method to assess whether dimerization is a requirement for catalytic activity, since it is unlikely that the active sites, which are separated from the interface by ~25 Å (Figure 2), will be severely affected by possible structural changes induced by mutagenesis of the interface residues.

MATERIALS AND METHODS

Materials. All reagents were obtained from Sigma unless otherwise noted.

Site-Directed Mutagenesis. Site-directed mutagenesis of the pET17b/CK7 (*28*) plasmid containing the rmCK gene was carried out using the QuikChange kit (Stratagene) and a MJ Research PTC-200 Peltier thermalcycler. The only modification of the kit protocol was that transformation was performed using MAX efficiency DH5α competent *E. coli* cells (GIBCO Life Technologies). Mutagenic primers (Integrated DNA Technologies) were designed such that, in addition to changing the codon for the residue of interest, a restriction site was eliminated by a silent mutation. Single colonies of transformed cells were screened by restriction digest to identify those containing the desired mutant; then the plasmid DNA was isolated using a Qiagen plasmid purification kit. The entire gene was sequenced to confirm the desired mutation and to ensure that no other deleterious mutations were present. Sequencing was performed at the Ohio Agriculture Research and Development Center (Wooster, OH) using a Perkin-Elmer ABI377 automated instrument.

Protein Expression and Purification. Each mutant protein was overexpressed in BL21(DE3)pLys(S) *E. coli* cells (Promega). Cell cultures were grown at 37 °C in LB/ampicillin (100 μg/mL) /chloramphenicol (35 μg/mL) to an optical density of 0.6−0.8 AU, and IPTG was then added to a final concentration of 0.4 mM to induce protein synthesis and the culture was grown at 18.5 °C for 14−16 h. The cells were pelleted by centrifugation prior to protein purification. Wild-type enzyme was purified by methods described previously (*28*). The bacterial cells used to express mutant proteins were resuspended 10 mM MES, 40 mM KCl, 5 mM EDTA, 1 mM DTT, 0.1 mM PMSF, pH 6.0, containing 0.02 mg/mL DNase and lysed by sonication. The cell lysate was centrifuged at 40 000 rpm, and the CK was purified from the supernatant by affinity chromatography with a Cibracron Blue 3GA agarose column using a Pharmacia FPLC. The CK protein was eluted using 10 mM TES, pH 8.0, containing 40 mM KCl, 5 mM EDTA, 1 mM DTT, and 0.1 mM PMSF and was collected in fractions. Later fractions of a single elution peak were composed almost entirely of CK. These fractions were combined and concentrated to approximately 1.5 mL by ultrafiltration into 20 mM Tris, 0.1 mM EDTA, pH 8.0 (TE buffer). A small amount of DNAase (~0.2 mg) was added, and the solution was dialyzed against TE buffer using 10 000 MWCO dialysis cassettes (Pierce) to remove nucleotides. After affinity chromatography the CK mutants were found to be ~90−98% pure by SDS−PAGE (BioRad). Further purification of enzymes to >98% purity (necessary for spectroscopic experiments) was accomplished by size exclusion chromatography (see below). All purification steps were performed at 4 °C. Protein concentration was measured by absorbance at 280 nm ($\epsilon = 75\,600$ cm^{-1} M^{-1}) (*29*).

Size-Exclusion Chromatography (SEC). Prior to SEC proteins were exchanged into 20 mM Tris, 50 mM sodium acetate, 250 mM NaCl, 0.1 mM EDTA, pH 8.10 (SEC buffer), using a Millipore ultrafiltration unit. Aliquots (200 μL of 1 mg/mL protein solution) were injected onto a Pharmacia Superose 12 10/30 high-resolution size-exclusion column and eluted with SEC buffer at 4 °C at a flow rate of 1.0 mL/min. Protein elution was monitored by absorbance at 280 nm, and fractions were collected and analyzed by SDS−PAGE to confirm the presence and retention time of each CK protein. Molecular weights were estimated against calibration standards: β-amylase (200 kDa), alcohol dehydrogenase (150 kDa), BSA (66 kDa), egg ovalbumin (43 kDa), carbonic anhydrase (29.0 kDa), and cytochrome *c* (12.4 kDa).

Analytical Ultracentrifugation. Sedimentation equilibrium experiments were performed at the University of North Carolina-Chapel Hill Macromolecular Interactions Facility using a Beckman Optima XL-A instrument. Protein samples were prepared so that the absorbance was 0.50 au/cm^{-1} at 280 nm in 0.050 M sodium phosphate buffer pH 7.4. Each sample was sequentially equilibrated by centrifugation at 10 000, 14 000, and 20 000 rpm for 20−24 h at 25 °C. The samples were then run at 45 000 rpm for 6 h, and the background absorbance measured to correct the sedimentation profiles. The average, apparent molecular weight of each protein was calculated using eq 1 (*30*), where *c* is the molar concentration determine by absorbance, *r* is the radial distance, *M* is the average, apparent molecular weight, υ is specific molar volume (0.736 mL/g), ρ is the solution density (0.997 g/mL), ω is the radial velocity in rad^2/s^2, *T* is the temperature (K), and *R* is the gas constant (8.315×10^7 egs K^{-1} mol^{-1}):

$$\frac{\ln c}{r^2} = \frac{M(1 - \upsilon\cdot\rho)\omega^2}{2RT} \quad (1)$$

The molecular weight for the wild-type and mutant proteins was calculated using the data set from the rotation rate that would most accurately measure the predicted mass by having the broadest sedimentation profile across the measurement window.

Sedimentation equilibrium profiles were also used to calculate the dissociation constant, $K_{d(D\rightarrow M)}$, of the dimer/monomer equilibrium using a derivation of the Lamm partial differential equation (eq 2) that describes the movement of protein monomers and homodimers in a centrifugal field (*31*)

$$C_{total} = C_{ref}\varphi + 2K_{assoc}(C_{ref}\varphi)^2 \quad (2)$$

where C_{total} is the total protein concentration (μM) and ψ is experimentally determined from the sedimentation equilibrium profile using eq 3 (*32*), where r_0 is an arbitrary fixed radius reference:

$$\varphi = e^{\frac{M(1 - \upsilon\rho)\omega^2(r^2 - r_o^2)}{2RT}} \quad (3)$$

ANS Fluorescence Experiments. Mixtures of 2.0 μM protein subunit and 10 μM anilinonaphthalene-8-sulfonate (ANS) in TE buffer were measured using a SPEX FluoroLog fluorescence spectrometer. Excitation was carried out at 360 nm while the emission was measured from 390 to 600 nm using slit widths of 2 nm for both the excitation and emission monochromators. Samples were measured using quartz cells (1 × 1 cm) located in a temperature controlled sample holder. ANS fluorescence was measured as a function of temperature by preparing solutions containing 2.0 μM protein subunit and 10 μM ANS. The fluorescence was first measured at 25.0 °C and the temperature raised in 2.0 °C increments and a fluorescence emission spectrum obtained at each temperature plateau. All solutions were incubated for 15 min at a given temperature to allow thermal equilibration before obtaining a spectrum.

Enzyme Kinetics. Prior to all kinetics experiments, proteins were exchanged into TE buffer by ultrafiltration. Creatine kinase activity was determined at pH 9.00 and 30.0 °C in the direction of phosphocreatine formation using a pH stat assay described previously (*28*). The data were fit to a random-order, rapid-equilibrium, or sequential-ordered mechanism to determine kinetic and thermodynamic constants using the method developed by Cleland (*33*) using software written by Dr. Ronald E. Viola. Thermal inactivation was determined by incubating the CK solution for 10 min at fixed temperatures varying from 25 to 60 °C, then determining the specific activity using 1.6 mM MgATP and 100 mM creatine in a pH stat assay at 30.0 °C.

Guanidine Hydrochloride Denaturation. All denaturation experiments were carried in 100 mM Tris HCl, pH 8.00. Solutions were prepared containing 6 μM protein subunit and a variable amount of GdnHCl. The intrinsic protein fluorescence spectra were measured at 25 °C, with excitation at 290 and 1.0 nm slit widths.

RESULTS

Five dimer interface mutants—the R147A, R151A, and D209A single mutants, the R147A/R151A double mutant, and the R147A/R151A/D209A triple mutant—were prepared and confirmed to be free of spurious mutations by DNA sequencing. Each of the resulting proteins was successfully overexpressed in *E. coli*, but none could be purified using the same procedure as the WT enzyme, which involves affinity chromatography on Blue Sepharose followed by anionic exchange chromatography (*28*). The triple mutant was overexpressed as insoluble inclusion bodies which could not be resolublized, and subsequent experiments involving this mutant were discontinued. Each of the other four mutants was soluble and was successfully purified by affinity chromatography; however, anion exchange was unsuccessful in each instance. Instead, size-exclusion chromatography on Superose 12 was used as the second chromatographic step to generate mutant CK solutions that were >98% pure, as determined by SDS−PAGE. Precipitation of the R147A/R151A protein was noted during prolonged exposures to elevated temperatures (T>26 °C); thus, all preparations and manipulations of this mutant were performed at 4 °C.

Size Exclusion Chromatography. SEC was used to examine the quaternary structure of each mutant compared to the WT enzyme. Each protein had a different chromatographic profile (Figure 3), with a major peak and a shoulder at shorter retention time suggesting a small amount of higher molecular weight aggregate. The order of elution was WT < R151A < D209A < R147 ≈ R147A/R151A. Using a set of molecular weight standards, the apparent molecular weight of each protein was calculated (Table 1) by plotting log(molecular weight) versus retention time. These data indicate that at the concentrations measured ([CK] = 1 mg/mL injected) WT and R151A exist in the dimeric form, R147A and R147A/R151A are monomeric, while the D209A appears to be in an equilibrium mixture of dimer and monomer.

To determine the effect of concentration on the R147A/R151A quaternary state, 2 and 5 mg/mL samples were injected onto the size-exclusion column and gave calculated molecular weights of 47 and 49 kDa, respectively. The higher values may be due to a shift of the monomer/dimer equilibrium toward the formation of small amounts of dimer. Heterodimer formation between WT and R147A/R151A was tested by injecting a mixture (1 mg/mL each) of both proteins. Two peaks were observed with retention times and

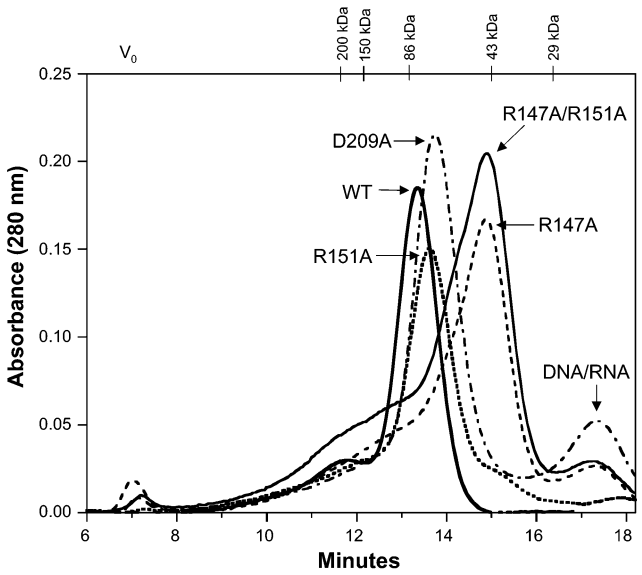

FIGURE 3: Size-exclusion chromatograms of the WT and dimer interface mutants. The corresponding molecular weight scale calculated from the retention time of the molecular weight standards is given on the top axis.

Table 1: Apparent Molecular Weights as Determined by Size-Exclusion Chromatography and Analytical Untracentrifugation

	apparent molecular weight		
enzyme	size exclusion chromatography[a]	AUC[b]	dimer/monomer $K_{d(D\rightarrow M)}$ (μM)[c]
WT	85 kDa	86 kDa[d]	0.05 ± 0.03
R147A	46 kDa	42 kDa[e]	33.4 ± 1.2
R151A	81 kDa	67 kDa[d]	5.0 ± 0.5
D209A	74 kDa	71 kDa[f]	3.8 ± 0.7
R147A/R151A	45 kDa	45 kDa[e]	45.5 ± 8.3
R147A/R151A/D209A	insoluble aggregate formed on expression		

[a] The apparent molecular weight was calculated by comparison of retention times to data obtained from molecular weight standards. [b] Molecular weights were calculated from analytical ultracentrifugation data using previously described methods (*30*). [c] Subunit dissociation constants at 25 °C were calculated using analytical ultracentrifugation data and methods described previously (*31*, *32*). Best fit data were obtained from either 10 000,[d] 14 000,[f] or 20 000[e] rpm centrifugation experiments.

Table 2: Kinetic Analysis of WT rmCK and the Dimer Interface Mutants[a]

	MgATP (mM)		creatine (mM)			relative	
enzyme	K_{dA}	K_{MA}	K_{dC}	K_{MC}	k_{cat} (s^{-1})	k_{cat} (s^{-1})	$k_{cat}/(K_{dA}K_{MC})$
WT[b]	0.90 ± 0.08	0.81 ± 0.17	8.3 ± 0.9	7.5 ± 1.5	104 ± 3.8	1.00	1.00
R147A[c]		39.3 ± 9.2	22.7 ± 6.4		11.7 ± 1.1	0.11	0.0085
R151A[d]	0.86 ± 0.05	1.22 ± 0.15	6.3 ± 0.4	8.8 ± 1.0	21.1 ± 0.4	0.20	0.18
R147A/R151A[d]	15.8 ± 4.7	8.2 ± 2.6	76 ± 24	39 ± 12	62 ± 12	0.60	0.0065

[a] MgATP = A; creatine = C. [b] Wild-type data taken from (*18*) and fit to a random-order rapid-equilibrium mechanism. [c] Set of initial rates could only fit to a ordered mechanism where creatine binds first. [d] Data fit to random-order rapid-equilibrium mechanism.

areas corresponding to the pure individual samples, indicating that heterodimers were not generated under these conditions.

Analytical Ultracentrifugation. The quaternary structure of each protein was also assessed using sedimentation equilibrium experiments. The initial concentration of the protein used in these experiments was 0.6 mg/mL, approximately half that used for SEC. In general, the results obtained by AUC (Table 1) are comparable to those obtained by SEC and confirm that the R147A and R147A/R151A mutants are monomers. The only inconsistency between the two data sets was that the R151A molecular weight determined by AUC was significantly lower in value; 62 versus 81 kDa for SEC. This was attributed to either SEC not being able to accurately determine the molecular weight or that the higher temperature necessary to perform sedimentation measurements (4 vs 25 °C) shifted the postulated monomer/dimer equilibrium toward the monomeric form.

Dissociation constants for the monomer/dimer equilibrium were measured from the sedimentation profiles. There is strong correlation between the quaternary state measured by both AUC and SEC and the value of the $K_{d(D\rightarrow M)}$ for monomer/dimer dissociation. The magnitude of the $K_{d(D\rightarrow M)}$ for the R147A/R151A mutant is consistent with the observation of minor amounts of dimer at higher protein concentrations, although the temperature difference between each experiment makes a definitive comparison impossible.

Kinetic Analysis. A kinetic analysis of the forward reaction (phosphocreatine formation) at 30 °C was carried out using 5 different creatine and MgATP concentrations in all combinations to generate a matrix of 25 individual initial rates. The rate data for the R151A, R147A/R151A, and native enzyme all fit well to a random-order, rapid-equilibrium mechanism characteristic of rmCK (*7*). The kinetic parameters measured for the R151A mutant are similar to those obtained for the native enzyme (Table 2). Specifically, the K_d and K_M values for each substrate are nearly identical within experimental error, with the only change being a 5-fold reduction in k_{cat}. For the two mutants shown to be monomers, R147A and R147A/R151A, the main effect of the change in quaternary state is a reduced affinity for MgATP and creatine (Table 2). The K_d values for the R147A/R151A mutant are approximately 1 order of magnitude higher than those of the WT. Once substrates are bound catalysis seems to be relatively unaffected as the k_{cat} is approximately 60% that of WT. Thus, the nearly 200-fold reduction in catalytic efficiency for the R147A/R151A mutant is largely due to an decrease in substrate affinity. Interestingly, the data for R147A could only be fit to an ordered binding mechanism in which creatine binds first. In addition, the R147A protein has significantly reduced affinity for both substrates: a ~4-fold reduction for creatine and ~50-fold reduction for MgATP. The catalytic efficiency of the R147A mutant is also reduced by a 10-fold reduction in k_{cat}, giving it a net efficiency of about 0.1% compared to WT.

Initial rates could not be measured for the D209A enzyme because the rate of hydrogen ion production rapidly decelerated during the first 10−20 s of the experiment. The change was not due a depletion in substrates and was attributed to dissociation of the more active dimeric form upon dilution into the reaction mixture. A concentration of the D209A protein could not be found which successfully eliminated the apparent dimer to monomer transition within the constraints of the pH stat experiment.

The pH stat technique lacks specificity in that it is sensitive to changes in hydrogen ion concentration regardless of the source of such changes. As a result, any ATPase activity (hydrolysis of MgATP in the active site) will also be measured and could be mistakenly attributed to kinase activity. Since the active site structure of these mutants may be significantly altered, perhaps leading to an increased accessibility to water, the ATPase activity of the WT and each of the mutants was measured at 1.0 mM MgATP as described previously (*34*). WT enzyme has an ATPase activity that is nearly 10^6 lower than its native kinase activity (ATPase: 4.8×10^{-5} μmol min^{-1} mg^{-1}; kinase: 6.3×10^{1} μmol min^{-1} mg^{-1}). The dimer interface mutants have ATPase activities that are significantly below their corresponding kinase activities (ratio ATPase/kinase activities: R147A, 2.4×10^{-5}; R151A, 1.3×10^{-6}; R147A/R151A, 1.3×10^{-6}). The D209A mutant had a ATPase activity of 2.6×10^{-5} μmol min^{-1} mg^{-1}, which was within 1 order of magnitude to the activities of the other mutants and the WT.

Thermal Inactivation. The thermal stability of the mutants and the WT enzyme was determined by incubation of samples at a specific temperature for 10 min followed by measurement of the activity at 30.0 °C. Figure 4 shows the relative activity (i.e., activity after incubation at the given temperature/ activity after incubation at 25 °C) as a function of the temperature of incubation. It should be noted the absolute activities of the individual enzymes are significantly different. The results indicate that WT rmCK retains its activity at elevated temperature much better than any of the mutants (Figure 4), losing activity between 53 and 55 °C. The monomeric mutants, R147A and R147A/R151A, undergo relatively gradual losses in activity across the temperature range used, with midpoints of inactivation of 41 and 37 °C, respectively. Likewise, the R151A mutant also exhibits a steep drop in activity at increasing temperatures, but the transition occurs at 40−43 °C. Protein aggregation was observed following the inactivation of R151A, as evidenced by a precipitate that formed under such conditions.

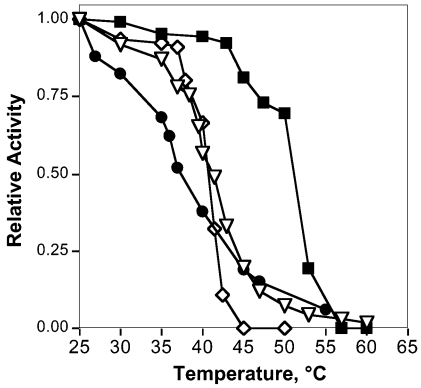

FIGURE 4: Thermal inactivation of the WT (■), R151A (◇), R147A (▽), and R147A/R151A (●) mutants as measured by the pH stat method. Relative activity for each protein is the ratio of the specific activity at given temperature divided by the specific activity measured after incubation at 25 °C. The error in each data point is approximately ±5%.

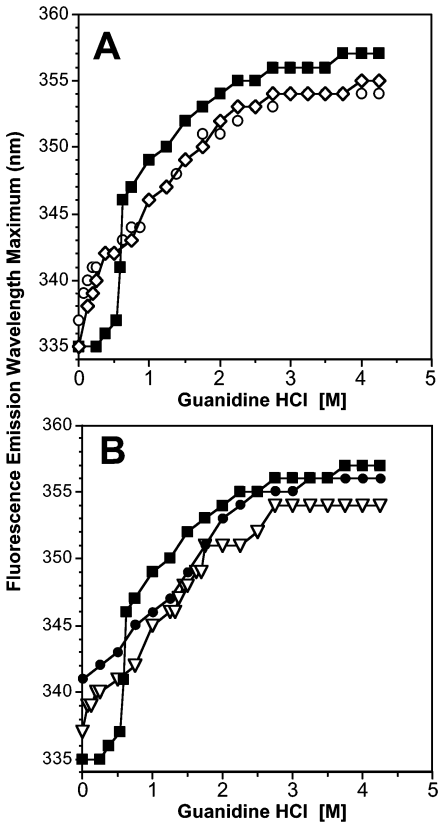

FIGURE 5: Intrinsic fluorescence emission maximum vs GdnHCl concentration. (A) WT (■), R151A (◇), and D209A (○). (B) WT (■), R147A (▽), and R147A/R151A (●).

The rapid drops in activity for both the R151A and native enzyme are attributed to a dimer → monomer transition which generates monomeric forms that have significantly reduced catalytic efficiency or are completely inactive.

GdnHCl Denaturation. Each subunit of rmCK contains four tryptophans at positions 210, 217, 227, and 272. The wavelength maximum of the intrinsic tryptophan fluorescence for each protein was determined as a function of GdnHCl concentration (Figure 5). GdnHCl denaturation of native rmCK as followed by intrinsic fluorescence has previously been measured (*35*−*37*), and the overall characteristics of the denaturation curve for WT obtained here match published data. As seen in Figure 5, the most dramatic change in the WT fluorescence maxima induced by increasing [GdnHCl] was an 11 nm bathochromic shift which occurs at approximately 0.6 M GdnHCl. As confirmed elsewhere by SEC−FPLC (*35*), this transition in the GndHCl denaturation curve has been attributed to dimer dissociation. A similar shift fluorescence maximum accompanying subunit dissociation has also been noted using NaCl and LiCl denaturants (*21*).

The greatest differences between the GdnHCl induced denaturation profiles among the five proteins measured occurs in the region from 0 to 1 M GdnHCl. Figure 5A shows that the R151A fluorescence maximum at 0 M GdnHCl is 335 nm like the WT but undergoes a red shift indicative of subunit dissociation at a significantly lower concentration of GdnHCl, ∼0.1 M. In addition, there appear to be two transitions occurring between 335 and 346 nm for R151A. This behavior indicates that R151A is dimeric, but is more susceptible to dimer dissociation by GdnHCl. The D209A mutant has a fluorescence maximum of 337 nm at 0 M GdnHCl, which is red shifted 2 nm compared to both WT and R151A. D209A also undergoes the apparent dimer → monomer transition at a GdnHCl concentration lower than 0.1 M. In contrast, the two monomeric mutants (R147A and R147A/R151A) have profiles which lack the initial bathochromic wavelength shift (Figure 5B). The λ_{max} of the R147/R151A in buffer alone is 341 nm, a maximum wavelength characteristic of a monomer (*35*). The R147A mutant has a somewhat shorter wavelength maximum in buffer, 337 nm, which red shifts to 340 nm at 0.12 M GdnHCl. This behavior may indicate that some degree of dimerization may be taking place in the absence of denaturant, a fact that is supported by the slightly larger apparent molecular weight determined by SEC.

At higher concentrations of GdnHCl a multistate sequential unfolding takes place that is relatively similar among all of the proteins measured. This unfolding profile is consistent among a mitochodrial isoform of CK (chicken sarcomeric, a 340 kDa octomer) and AK (lobster, a 40 kDa monomer), which indicates that these transitions are not a function of the oligomerization state but are common to guanidino kinases (*35*). The one deviation in the later part of the denaturation profiles is seen in the R147A curve (Figure 5B) from 2 to 3 M GdnHCl. In this concentration range, the λ_{max} of R147A initially remains relatively constant and then rapidly red shifts nearly 3 nm at about 2.75 M. The origin of this behavior is not obvious; nor is how this behavior relates to the changes observed in the catalytic mechanism.

As noted above, kinetic data for the D209A mutant could not be collected because an equilibrium mixture of both dimeric and monomeric forms apparently coexist in solution. Since the wavelength maximum of the tryptophan fluorescence is indicative of the quaternary state, the D209A fluorescence was measured as a function of protein concentration to determine the $K_{d(D\rightarrow M)}$ for subunit dissociation. At 30 °C the fluorescence maximum shifted from 337 to 341 nm over a concentration range of 20−0.02 μM (data not shown). Assuming this shift was solely due to changes in quaternary state, a $K_{d(D\rightarrow M)}$ of ∼5 μM for dimer dissociation was estimated from these data, a value which is consistent with a value measured by AUC (Table 1). This experiment was unsuccessful for other mutants, as protein concentrations

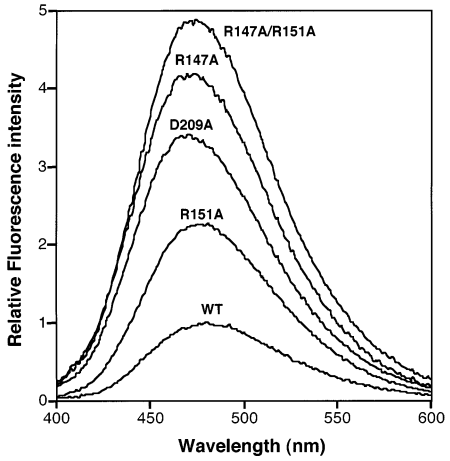

FIGURE 6: Normalized fluorescence spectra of solutions containing 10μM ANS and 2.0 μM of protein subunit. The fluorescence spectrum of 10 μM ANS in buffer measured under identical conditions was subtracted from each curve and the resulting data normalized so that the maximum WT fluorescence = 1.0.

needed to estimate these $K_{d(D\rightarrow M)}$ values were outside the dynamic range of the fluorescence measurement.

ANS Fluorescence. ANS has been used extensively as an extrinsic fluorescent probe of biological macromolecular structure (*38*−*40*). Since ANS is virtually nonfluorescent in polar solvents and exhibits a blue shift and significant increase in quantum yield when bound to hydrophobic regions on a protein (*41*), it can be used to investigate protein conformational changes. The normalized ANS fluorescence spectra observed when the probe is combined in a 5-fold molar excess ANS:protein subunit (5:1) are shown in Figure 6. The WT mixture has the lowest ANS fluorescence compared to all of the dimer interface mutants. Previous studies have shown that a single ANS molecule binds with high affinity in the nucleotide binding site of each subunit of native rmCK (*42*). ANS bound in this manner exhibits a λ_{max} of 488 nm (*42*), identical to the results for the WT seen here.

The ANS fluorescence intensities observed in Figure 6 can be correlated with the quaternary state of the mutant. For example, the greatest fluorescence intensity is observed when ANS is incubated with R147A/R151A. The R151A mutant, which has been shown to be principally dimeric, has an ANS spectrum that most closely resembles WT. To verify that the differences in the measured fluorescence spectra were not due to a difference in ANS binding affinity, the fluorescence of ANS was measured over a range of ANS:CK subunit molar ratios (1:1 to 500:1; the inner filter effect defined the upper limit). The data (not shown) indicate that the relative fluorescence intensity values became equivalent at ANS:CK mole ratios greater than 2:1, indicating that the differences are most likely due to an increase in the number of ANS binding sites.

Compared to changes seen in quantum yield caused by the polarity of the local environment, ANS fluorescence quantum yield is essentially insensitive to temperature (*43*, *44*). The fluorescence of solutions containing 10 μM ANS and 2.0 μM CK subunit were measured as a function of temperature in order to investigate possible conformational changes that occur upon thermal denaturation. The changes in ANS fluorescence are shown in Figure 7. Since all of the

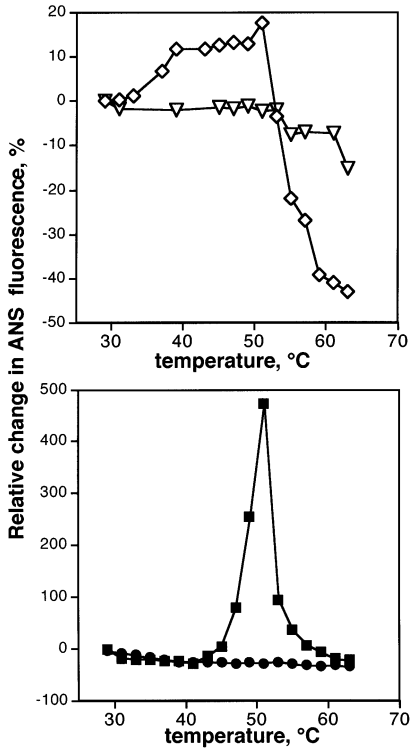

FIGURE 7: ANS fluorescence as a function of temperature. Each data point is the integrated fluorescence intensity of a mixture 10 μM ANS and 2.0 μM protein subunit minus the integrated ANS fluorescence in buffer. This difference was then normalized to the initial fluorescence measured at 25 °C. (A) R151A (◇) and R147A (▽). (B) WT (■) and R147A/R151A (●).

ANS/protein mixtures have different absolute intensities, fluorescence at a given temperature is plotted relative to the fluorescence measured at 25 °C. The behavior of the ANS fluorescence as a function of temperature for the proteins investigated can be grouped into two categories corresponding to quaternary state (dimer vs monomer). The dimeric proteins (R151A and WT) show an increase in fluorescence at approximately the same temperature that thermal inactivation of enzyme activity occurs (compare Figures 4, and 7A,B). After reaching a maximum value, the ANS fluorescence for the R151A and WT both markedly decrease at 52−58 °C. In contrast, the ANS fluorescence versus temperature profiles for the monomeric mutants (R147A and R147A/R151A) systematically decrease as the temperature increases. Measurement of the D209A mutant (data not shown) yielded a temperature profile that also showed a gradual decrease in fluorescence as the temperature increased that was roughly equivalent to the R147A curve.

DISCUSSION

Residues Important for Quaternary Structure. Using site-directed mutagenesis, we have selectively and systematically eliminated hydrogen bonding interactions made by the R147, R151, and D209 residues located in one-half the dimer interface of rmCK. These three residues were deemed to have significant importance, as they are fully conserved in all CKs and are each involved in multiple hydrogen bonds within and across the dimer interface. On the basis of the results obtained from SEC and sedimentation equilibrium experiments (Table 1), the quaternary state at ∼1 mg/mL is as follows: R151A, dimer; D209A, equilibrium mixture of

dimer and monomer; R147A, primarily monomer; and R147A/R151A, monomer. These results suggest that R147 is the residue that is most critical for dimer cohesion, since any mutation of this arginine to alanine leads to a monomeric species. On the basis of analysis of the crystal structure, the primary importance of R147 may be explained since it is the central amino acid of the triad of amino acids comprising that half of the interface, making two hydrogen bonding interactions across the interface to an aspartate and backbone carbonyl, and it may help organize the D209 in the same subunit through a hydrogen bond to the side chain carboxylate (Figure 1). The later interaction may, in part, explain the importance of D209, since its mutation to an alanine leads to a protein that is a mixture of dimers and monomers under equivalent experimental conditions. Despite R151's ability to form three hydrogen bonds across the dimer interface, the R151A mutation led to a protein that was primarily dimeric, suggesting the role of R151 in dimerization is less important. Thermal inactivation (Figure 3) and GdnHCl denaturation experiments (Figures 4) show that the R151A mutant dissociates into monomers under less harsh conditions compared to WT, indicating that the interactions facilitated by R151 do play a role in dimer stability.

Effect of Quaternary State on Catalysis. It was found that all of the mutants showed some degree of catalytic activity regardless of quaternary state. The fact that the monomeric mutants R147A/R151A and R147A are active clearly demonstrates that dimerization is not a prerequisite for enzymatic activity for rmCK. However, the monomeric mutants differ from the native enzyme in that the affinity for both substrates is significantly reduced (Table 2), which may indicate that changes in tertiary structure occur that affect substrate binding. This hypothesis is supported by the increase in ANS fluorescence observed for R147A/R151A and R147A mutants (Figure 6), a result that is indicative of the generation of exposed hydrophobic regions in these proteins. The fact that expression of R147A/R151A/D209A mutant resulted in an insoluble aggregate gives further anecdotal evidence that structural changes take place when such mutations are made. Several studies indicate that conformational changes take place upon binding of substrates to CK (*45*−*48*). In addition, the X-ray crystal structure of the horseshoe crab AK with a bound transition state analogue complex (*49*) shows that the flexible loop conserved among all guanidino kinase folds over the active site when substrates are bound (*50*). If these reported conformational changes are important to substrate binding, they may be hindered by any structural changes that may take place upon formation of the monomer. Interestingly, once substrates are bound catalysis is not greatly affected; i.e., k_{cat} for the R147A/R151A is 60% of WT and suggests that active site organization is intact.

The data for the R147A mutant could only be fit to an ordered kinetic mechanism in which creatine binds first. Even after creatine is bound, the affinity for MgATP is decreased 50-fold compared to WT. In contrast, k_{cat} is only reduced by a factor of 10 relative to the native enzyme, which again indicates that after substrates are bound catalysis is not prohibited. Overall, the R147A mutant has approximately 0.1% of the catalytic efficiency of native rmCK, similar to the R147A/R151A. On the basis of ANS fluorescence measurements, it is likely that the changes in enzymatic activity are again due to changes in tertiary structure. Since the R147A single site mutation can be considered a localized change in the protein far removed from the active site, it may be concluded that the structural changes affecting binding may be due to the subsequent formation of the monomer. The R151A mutant, which was found to be primarily dimeric, had measured K_d and K_M values for both substrates that were statistically indistinguishable from those of the native enzyme, although k_{cat} was reduced 5-fold. The reasons for the reduction in k_{cat} are not understood.

Effect of Quaternary State on Stability. Loss of enzyme activity of each mutant protein at elevated temperatures and unfolding by use of chemical denaturants were used to assess the relative global and local stability, respectively. The GdnHCl denaturation data show significant differences in the intrinsic fluorescence at low concentrations of denaturant. For reasons noted above, these difference are attributed to changes in quaternary state, not to gross unfolding. At higher concentrations of GdnHCl, the changes in intrinsic fluorescence of the mutants are, for the most part, identical to WT. The only notable difference is observed with the R147A mutant in the region from 2 to 3 M GdnHCl. There is a significant transition by the R147A at about 2.75 M GdnHCl, while the other proteins exhibit a more gradual shift in fluorescence maximum in this region; yet all show a distinct yet smaller jump at about 2.75 M. The overall consistency of the profiles suggests that the unfolding pathways in the WT and mutants are very similar or nearly equivalent, with perhaps the exception of the R147A mutant.

There were significant changes in the thermal inactivation profiles of the mutants compared to WT (Figure 4). It was found that the native enzyme retained nearly full activity until 45 °C, which was followed by a slow decrease in activity until 55 °C when the activity sharply declined. Work by other investigators using circular dichroism (*28*) and differential scanning calorimetry (*51*) have shown that rmCK exhibits a significant loss of secondary structure and thermodynamic unfolding at approximately 56 °C. The monomeric R147A and R147A/R151A mutants, lost activity at significantly lower temperatures. Midpoints of the activity losses occurred at 42 °C for R147A and 37 °C for R147A/R151A, indicating a substantial reduction in structural stability for these proteins. The R151A mutant, which has an absolute specific activity much greater than the monomeric mutants, has a thermal inactivation profile similar in shape to WT, but complete inactivation occurs at a temperature 10 °C lower than WT. A steep drop in R151A activity around 40−45 °C compared to the monomeric mutants' profiles (Figure 5) may be indicative of the thermal dissociation of the dimer. An increase in ANS fluorescence at the same temperature where loss of activity is noted suggests that new hydrophobic surfaces are exposed at the point of activity loss (Figure 7A). On the basis of analysis of the rmCK X-ray crystal structure (*15*), few hydrophobic residues are exposed to solvent upon dimer dissociation, which is not surprising given the limited amount of contact between the two subunits. The regions exposed to solvent upon subunit dissociation may in some cases be the contact sites themselves, since replacement of Arg or Asp by alanine mutations would lead to a slightly more nonpolar surface. On the other hand, loss of the subunit-subunit contacts may lead to conformational changes leading to exposure of hydrophobic

regions, a possibility supported by the kinetic and spectroscopic data obtained for the monomeric mutants.

Measurement of ANS fluorescence as a function of temperature (Figure 7A,B) shows that no new ANS binding sites seem to be generated as the R147A and R147A/R151A monomeric mutants lose activity. Instead, a steady loss in ANS fluorescence attributed to thermal dissociation of ANS is observed. For both the R151A and WT, proteins a substantial drop in ANS fluorescence is seen at approximately 55 °C and may indicate that the additional ANS binding sites formed upon dimer dissociation during thermal inactivation are lost.

Conclusions. Size-exclusion chromatography, analytical ultracentrifugation, and intrinsic fluorescence measurements are self-consistent in showing that a monomer of rmCK has been prepared using site-directed mutagenesis, with the key residue in dimer formation being R147. Kinetic analysis of the monomeric forms of rmCK has shown that enzymatic activity is not precluded in disruption of the dimer, although substrate binding seems particularly sensitive to the quaternary state, perhaps because of structural changes that take place in the monomeric species. The thermal stability of the mutants in the monomeric state is significantly reduced. Unfolding by chemical denaturation seems to occur through a similar pathway to that of WT, indicating that the overall tertiary structure is relatively unchanged.

ACKNOWLEDGMENT

We thank Dr. Ashutosh Tripathy at the University of North Carolina, Chapel Hill, for assistance with the sedimentation equilibrium experiments.

REFERENCES

1. Dawson, M., Eppenberger, H. M., and Kaplan, N. O. (1965) *Biochem. Biophys. Res. Commun. 21*, 346−353.
2. Kuby, S. A., Noda, L., and Lardy, H. A. (1954) *J. Biol. Chem. 209*, 191−201.
3. Watts, D. C. (1973) in *The Enzymes* (Boyer, P. D., Ed.) Vol. 8, pp 383−455, Academic Press, New York.
4. Kenyon, G. L., and Reed, G. H. (1983) *Adv. Enzymol. 54*, 367−426.
5. Walliman, T., Wyss, M., Brdiczka, D., Nicolay, K., and Eppenberger, H. M. (1992) *Biochem. J. 281*, 21−40.
6. Bickerstaff, G. F., and Price, N. C. (1978) *Int. J. Biochem. 9*, 1−8.
7. Morrison, J. F., and James, E. (1965) *Biochem. J. 97*, 37−52.
8. Morrison, J. F. (1973) in *The Enzymes*. (Boyer, P. D., Ed.) Vol. 8, pp 457−486, Academic Press, New York.
9. Ellington, W. R. (2001) *Annu. Rev. Physiol. 63*, 289−325.
10. Muhlebach, S. M., Gross, M., Wirz, T., Wallimann, T., Perriard, J.-C., and Wyss, M. (1994) *Mol. Cellu. Biochem. 133/134*, 245−262.
11. Suzuki, T., and Furukohri, T. (1994) *J. Mol. Biol. 237*, 353−357.
12. Suzuki, T., Kawasaki, Y., Furukohri, T., and Ellington, W. R. (1997) *Biochim. Biophys. Acta 1348*, 152−159.
13. Suzuki, T., Kawasaki, Y., Unemi, Y., Nishimura, Y., Soga, T., Kamidochi, M., Yazawa, Y., and Furukohri, T. (1998) *Biochim. Biophys. Acta 1388*, 253−259.
14. Stein, L. D., Harn, D. A., and David, J. R. (1990) *J. Biol. Chem. 265*, 6582−6588.
15. Rao, J. K. M., Bujacz, G., and Wlodawer, A. (1998) *FEBS Lett. 439*, 133−137.
16. Webb, T. I. and Morris, G. E. (2001) *Proteins: Struct., Funct., Genet. 42*, 269−278.
17. Perraut, C., Clottes, E., Leydier, C., Vial, C., and Marcillat, O. (1998) *Proteins 32*, 43−51.
18. Edmiston, P. L., Schavolt, K. L., Kersteen, E. A., Moore, N. R., and Borders Jr., C. L. (2001) *Biochim. Biophys. Acta 1546*, 291−298.
19. Bickerstaff, G. F. and Price, N. C. (1976) *FEBS Lett. 64*, 319−321.
20. Grossman, S. H., Pyle, J., and Steiner, R. J. (1981) *Biochemistry 20*, 6122−6128.
21. Couthon, F., Clottes, E., and Vial, C. (1997) *Biochim. Biophys. Acta 1339*, 277−288.
22. Couthon, F., Clottes, E., Angrand, M., Roux, B., and Vial, C. (1996) *J. Protein Chem. 15*, 527−537.
23. Couthon, F., Clottes, E., Ebel, C., and Vial, C. (1995) *Eur. J. Biochem. 234*, 160−170.
24. Leydier, C., Clottes, E., Couthon, F., Marcillat, O., Ebel, C., and Vial, C. (1998) *Biochemistry 37*, 17579−17589.
25. Zhou, H.-M., Zhang, X.-H., Yin, Y., and Tsou, C. L. (1993) *Biochem. J. 291*, 103−107.
26. Zhou, J.-M., Zhu, L., and Balny, C. (2000) *Eur. J. Biochem. 267*, 1247−1253.
27. Lin, Z., and Zhou, J. (1995) *Biochim. Biophys. Acta 1253*, 63−68.
28. Chen, L. H., Borders Jr., C. L., Vasquez, J. R., and Kenyon, G. L. (1996) *Biochemistry 35*, 7895−7902.
29. Noda, L., Kuby, S. A., and Lardy, H. (1953) *J. Am. Chem. Soc. 75*, 913−917.
30. Williams, J. W., van Holde, K. E., Baldwin, R. L., and Fujita, H. (1958) *Biophys. J. 36*, 575−588.
31. McRorieD. K. and Volker, P. J. (1993) *Self-Associating Systems in the Analytical Centrifuge*, Beckman Instruments, Palo Alto, CA.
32. Wills, P. R., Jacobsen, M. P. and Winzor, D. J. (1996) *Biopolymers 38*, 119−130.
33. Cleland, W. W. (1979) *Methods Enzymol. 63*, 103−138.
34. LeBel, D., Poirier, G. G., and Beaudoin, A. R. (1978) *Anal. Biochem. 85*, 86−98.
35. Gross, M., Lustig, A., Wallimann, T., and Furter, R. (1995) *Biochemistry 34*, 10350−10357.
36. Clottes, E., Leydier, C., Couthon, F., Marcillat, O., and Vial, C. (1997) *Biochim. Biophys. Acta 1338*, 37−46.
37. Fan, Y. X., Zhou, J. M., Kihara, H., and Tsou, C. L. (1998) *Protein Sci. 12*, 2631−2641.
38. Brand, L., and Gohlke, J. R. (1972) *Annu. Rev. Biochem. 41*, 843−868.
39. Weber, L. D., Tulinsky, A., Johnson, D. J., and El-Bayoumi, M. A. (1979) *Biochemistry 18*, 1297−1303.
40. Salvik, J. (1982) *Biochim. Biophys. Acta 694*, 1−25.
41. Edelman, G. M., and McClure, W. O. (1967) *Acc. Chem. Res. 1*, 65−70.
42. McLaughlin, A. C. (1974) *J. Biol. Chem. 249*, 1445−1452.
43. Gally, J. A., and Edelman, G. M. (1965) *Biochim. Biopys. Acta 94*, 175−182.
44. Andley, U. P., and Chakrabarti, B. (1981) *Biochemistry, 20*, 1687−1693.
45. Samuels, A. J., Nihei, T., and Noda, L. (1961) *Proc. Natl. Acad. Sci. U.S.A. 47*, 1992−1996.
46. Morris, G. E., and Man, N. T. (1992) *Biochim. Biophys. Acta 1120*, 233−238.
47. Forstner, M., Kriechbaum, M., Laggner, P., and Wallimann, T. (1998) *Biophys. J. 75*, 1016−1023.
48. Granjon, T., Vacheron, M.-J., Vial, C., and Buchet, R. (2001) *Biochemistry 40*, 2988−2994.
49. Zhou, G., and Somasundaram, T. (1998) *Proc. Natl. Acad. Sci. U. S. A. 95*, 8449−8454.
50. Zhou, G., Ellington, W. R., and Chapman, M. S. (2000) *Biophys. J. 78*, 1541−1550.
51. Lyubarev, A. E., Kurganov, B. I., Orlov, V. N., and Zhou, H.-M. (1999) *Biophys. Chem. 79*, 199−204.

BI027083B